The antimicrobial peptide Temporin L impairs *E. coli* cell division by interacting with FtsZ and the divisome complex

Angela Di Somma,[1#] Concetta Avitabile,[2#] Arianna Cirillo,[1] Antonio Moretta,[3] Antonello Merlino,[1] Luigi Paduano,[1] Angela Duilio[1*] and Alessandra Romanelli[4*]

[1] Department of Chemical Sciences, University of Naples "Federico II"
Via Cinthia 4, 80126 Napoli, Italy

[2]Institute of Biostructures and Bioimaging (CNR), via Mezzocannone 16, 80134 Napoli, Italy

[3]Department of Sciences, University of Basilicata, Potenza Italy

[4]Department of Pharmaceutical Sciences, University of Milan, Via Venezian 21, 20133, Milan (Italy)

[#] These authors equally contributed to the work
*: co-corresponding authors

Running title: Temporin L inhibits *E.coli* cell division

Keywords: Temporin L; FtsZ; proteomics; cell division; inhibitor; antimicrobial; peptide; SANS

ABSTRACT

The comprehension of the mechanism of action of antimicrobial peptides is fundamental for the design of new antibiotics. Studies performed looking at the interaction of peptides with bacterial cells offer a faithful picture of what really happens in nature. In this work we focused on the interaction of the peptide Temporin L with *E.coli* cells, using a variety of biochemical and biophysical techniques. Functional proteomic studies allowed us to identify bacterial proteins specifically interacting with the peptides that belong to the divisome machinery. Sequence homology suggested that the GTPase FtsZ is the specific peptide target. Docking experiments supported the FtsZ-TL interaction; binding and enzymatic assays using recombinant FtsZ confirmed this hypothesis and revealed a competitive inhibition mechanism. Optical microscopy and TEM measurements demonstrated that upon incubation with the peptide bacterial cells are unable to divide forming long necklace-like cell filaments. Dynamic light scattering studies and Small Angle Neutron Scattering experiments performed on treated and untreated bacterial cells, confirmed a non-membrano-lytic mechanism of action of our peptide and further indicated a change at the nanoscale level of the bacterial membrane.

INTRODUCTION

The growing demand of new antibiotics active against multi-resistant bacteria has encouraged the research of antimicrobial agents from natural sources. Peptides are the most common weapon that organisms from all domains of life produce to prevent the invasion by external pathogens. Antimicrobial peptides (AMPs) are short peptides consisting of 10-50 amino acids, often containing multiple hydrophobic and positively charged residues (1). Unlike common antibiotics, AMPs, alone and in combination with other antibiotics, are less prone to trigger resistance or transient cross-resistance and mainly act against bacterial cells (2, 3).

However, the possible exploitation of AMPs as new antibacterial drugs is strictly dependent on a clear description of their mechanism of action at the molecular level. Several studies focused on the interaction of antimicrobial peptides with Gram negative bacterial cells contributed to clarify some details on the mechanism of action of AMP (4). These studies indicated the chemical /physical features of bacteria and peptides that are fundamental for their interactions and which pathways, essential for the bacterial cell life, are affected by AMPs. Fluorescence microscopy studies on *E. coli* cells revealed that the kinetic of bacterial cell death is related to the composition of the lipopolysaccharide (LPS) (5). The interaction of peptides with LPS often triggers the folding of peptides (6, 7). A huge number of peptides covers the outer membrane of bacteria, determining its neutralization, as revealed by Z potential measurements (8, 9). Recently, single cell time-resolved fluorescence microscopy studies suggested that cationic AMPs initially permeabilize the outer membrane (OM) enabling a rapid access of the peptide to the periplasm. As the concentration of the peptide in the periplasm grows, the same process occurs to the cytoplasmic membrane, which is permeabilized only after the outer membrane is resealed, allowing AMPs to travel into the cytoplasm and generating a variety of possible damaging events downstream (10).

Protein targets of AMPs are currently deeply investigated, and it is now clear that different peptides may have different targets. Processes that have been found to be hampered by AMPs include bacterial cell division and outer membrane biogenesis. Inhibition of cell division is suggested when bacterial cells form elongated structures in the presence of antimicrobial peptides. Studies on the peptide C18G demonstrated that it impairs cell division in *E.coli* by interacting with the transmembrane protein PhoQ that

phosphorylates PhoP triggering the over-expression of the protein QueE that in turn blocks the divisome complex (11). Inhibition of outer membrane biogenesis yields defect in the architecture of the membrane. A combination of fluorescence microscopy, mass spectrometry and bioinformatics analyses demonstrated that the peptide thanatin affects the LPS transport machinery by interacting with both the periplasmic protein LptA and the outer membrane protein LptD (12).

LptD was also identified as the target of the peptidomimetic L27-11, which is specifically active on *P. aeruginosa* (13). Furthermore, a 15 amino-acid peptide fragment derived from BamA was demonstrated to have potent antibiotic activity being able to bind BamD, that is part of the complex devoted to the assembly of beta barrel proteins in the outer membrane of *E.coli* (14). These results suggest that AMPs may interact with either bacterial membrane or specific intracellular protein targets thus affecting cellular mechanisms and that a deeper investigation is essential for the definition of their effect on vital cellular processes.

We investigated the mechanism of action of the peptide Temporin L (TL) (15) a natural peptide secreted from the skin of the European frog *Rana temporaria* active against Gram positive and Gram-negative bacteria on *E. coli* cells. Functional Proteomic experiments indicated specific interaction of TL with proteins belonging to the divisome complex. Sequence homology alignment with other AMPs suggested a possible direct interaction with the GTPase FtsZ. Docking experiments supported the FtsZ-TL interaction that was clearly demonstrated by binding and enzymatic assays using recombinant FtsZ revealing a competitive inhibition mechanism. Optical microscopy and TEM measurements demonstrated that upon incubation with the peptide bacterial cells are unable to divide forming long necklace-like cell filaments. Finally, the effect of the peptide on the morphology and the structure of bacterial cells at nanoscale level was also investigated by both Ultra Small-Angle Neutron Scattering (USANS) and Small-Angle Neutron Scattering (SANS).

RESULTS

Effect of Temporin L on E. coli cell growth

The antimicrobial activity of TL was verified by monitoring *E. coli* cells growth in the presence of different concentrations of TL. The MIC was calculated to be 16 μM, in agreement with literature data (15). (Supplementary Figure 1)

Pull-Down experiment

A detailed investigation of the mechanism of action of TL at the molecular level was pursued by functional proteomics approaches. Biotinylated TL was immobilized onto streptavidin-conjugated agarose beads and incubated with a membrane protein extract from *E. coli* cells. The proteins specifically interacting with the peptide bait were eluted and digested with trypsin. The resulting peptide mixtures were directly analyzed by LC-MS/MS and the mass spectral data used to search a protein database using an in-house version of the Mascot software leading to protein identification. Proteins that were identified both in the control and in the sample were discarded, whereas those solely occurring in the sample and absent in the control were considered as putative TL interactors.

Figure 1A shows the distribution of TL putative protein partners according to their cellular localization and the biological processes they are involved into. A bioinformatic analysis was performed using the String software and the KEGG pathway showing that a large number of proteins gathered within a network involved in cell division and the biosynthesis of peptidoglycan for the production of the division septum (Figure 1B).

In particular, several proteins belonging to the divisome complex were identified including FtsZ, FtsA, MurG, MukB and MreB.

Among these proteins, FtsZ protein, is a bacterial tubulin homolog and is responsible of the Z ring formation, the first step in the formation of the divisome complex, which is responsible of the cell division. Recently, FtsZ was reported to be the target of two peptides, CRAMP (16-33) and MciZ (16). Sequence alignment showed that TL shares a high sequence homology to the C-terminal portion of both CRAMP (16-33) and MciZ (Figure 2A). This observation urged us to investigate the interaction of TL with FtsZ *in*

vitro and *in vivo* and to develop a molecular model of the peptide-protein interaction by docking calculations.

Docking experiments

The putative structural basis of the binding of TL to FtsZ were investigated by a docking study (Figure 2B). Calculations reveal that TL may bind the cavity that allows the accommodation of GDP in the structures of FtsZ from *B. subtilis* and *P. aeruginosa* (Figure 2C), thus suggesting a possible competitive inhibition of the peptide for the GTPase activity of the protein. A detailed analysis of the interactions at the protein/peptide interface suggests the involvement of hydrophobic and coulombic interactions, with Phe and Trp residues of the peptide that pack against residues Gly20, Gly21, Gly71, Ala72, Gly105, Gly106, Gly107 and Phe182 of the protein and with the side chain of the Arg of the peptide that could make a salt bridge with the side chain of Glu138 of Ftsz (Figure 2D).

Binding experiments

As docking calculations suggested a possible interaction between TL and FtsZ, we were stimulated to confirm the binding of the peptide TL to the protein FtsZ on experimental basis. A recombinant form of FtsZ was produced in *E.coli*, purified and used in binding and enzymatic assays. Fluorescence experiments were carried out using the peptide labeled at the N-terminus with fluoresceine incubated with increasing concentrations of the protein (Figure 3A). Data from Fig. 3A allowed us to calculate a Kd value of 17.4± 0.8 nM.

Enzymatic assays

To further validate the docking predictions and to study the effect of TL on FtsZ, the GTPase activity of the recombinant protein was assayed in the absence and in the presence of TL. The purified recombinant protein was incubated with GTP in the presence of the peptide (35 μM) and the GTPase activity of FtsZ was monitored in comparison with the untreated protein at different GTP concentrations. In the presence of TL a decrease in the enzymatic activity of FtsZ was clearly observed confirming a specific interaction of the peptide with FtsZ (Fig. 3B). Kinetic parameters were calculated

showing an increase of K_M by about 50% (112.0 μM as compared to 56.6μM in the absence of the peptide) whereas V_{max} remained unchanged, demonstrating the competitive inhibitory mechanism exerted by TL on FtsZ.

Optical microscopy and TEM analyses

The morphologic effect of FtsZ inhibition by TL on cell division was investigated *in vivo* by both optical microscopy measurements and TEM analyses. on *E. coli* cell cultures grown in the presence and in the absence of the peptide. Optical microscopy images clearly show that in the presence of TL (Fig. 4B) *E. coli* cells form long necklace-like structures containing a large number of *E.coli* cells originated by impairment in cell division that were absent in the control (Fig. 4A).

The TL effect on *E.coli* cells growth was also investigated by TEM analyses. TEM images shown in Fig 5B confirmed that following treatment with TL bacterial cells division was impaired as indicated by several cells bound together and unable to divide when compared to the control (Fig. 5A). No damage of membranes was detected and the cells appeared turgid.

Spectroscopic investigations

The large structures formed by *E. coli* cells upon treatment with TL were further investigated by static light scattering experiments. As shown in Fig. 6, at small values of the scattering vector q, in the range probed by the LS, the scattering intensity profile decays with a q^{-1} power low for the sample of *E. coli* cells in the presence of TL, whereas it remains essentially constant for the pure bacteria, i.e for the cells in the absence of the peptide. This suggests that, in the presence of TL, large elongated structures are formed with a length larger than 6000 nm, the limit of LS instrument.

SANS analysis revealed that a significant difference between untreated and treated *E. coli* cells occurs in the range between 20 nm (q= 0.001 A^{-1}) and 60 nm (q = 0.003 A^{-1}). In such range, the profile of the scattering intensity of *E. coli* cells changes drastically upon TL addition. In the presence of the peptide, the scattering intensity is higher than that collected for the system containing only the bacterium cells.. Furthermore, in this later a shoulder in the I(q) vs q is present, whereas in the system containing TL the shoulder disappears and the scattering intensity decreases with a greater slope.

DISCUSSION

Elucidation of the mechanism of action of antimicrobial peptides requires the identification of the peptide targets in bacterial cells. We investigated the mechanism of action of Temporin L by a functional proteomic approach based on pull-down experiments using a biotinylated version of the peptide as a bait to identify its specific protein targets in *E.coli*. It is well known that in the cell many processes are governed by the rapid and transient association of proteins in multicomponent functional complexes (17-19). In bacterial membranes, several proteins are embedded in complexes with cytoplasmic proteins. For example, the protein machine devoted to the transport of LPS spans from the periplasm to the outer membrane. Accordingly, the proteomic experiment led to the identification of several proteins belonging to a multicomponent complex extending from the cytoplasm to all three layers of the cell envelope known as the divisome complex involved in the cell division process.

Among the identified proteins, FtsZ, FtsA, MurG, MukB and MreB are known to assemble into a tightly regulated cellular machinery operating to safely separate the cell into two daughter cells by a two steps mechanism. FtsZ is a bacterial tubulin homolog, expressed in either Gram positive and Gram negative cells responsible of the first step in the division of bacterial cells. FtsZ polymerizes in filaments using GTP molecules to generate a ring-like structure, the Z ring, at the site of division (16), then recruits other proteins to assemble the divisome complex driving the construction of the cell envelope (20). In *E. coli,* FtsZ is tethered to the membrane through FtsA. MurG is a glycosyltranferase located in the lateral cell wall and at the division site that catalyzes the synthesis of peptidoglycan. Den Blaauween et al suggested the involvement of MurG in a complex containing several proteins, including FtsA, implicated in cell division (21). Immunoprecipitation experiments demonstrated that MurG is also associated with MreB. MreB is essential for the maintenance of cell shape and plays a key role in cell division, being recruited to the septum upon direct interaction with FtsZ (22), an interaction functional to Z ring contraction.

Recently, *Bacillus subtilis* cells were reported to form filamentous structures upon incubation with the peptide CRAMP 16-33 and the interaction of the peptide with FtsZ

was proposed to be responsible of this phenomenon and the following bacterial cell death (16). Sequence alignment showed that TL displays high sequence homology with CRAMP and with the C-terminus of MciZ protein, a small protein of 40 amino acids known to be the physiological inhibitor of FtsZ. Based on these data, we investigated the possible interaction of TL with FtsZ. Docking simulation revealed that TL may bind FtsZ in the GTP binding site, thus suggesting a possible competitive inhibition mechanism of the peptide for the GTPase activity of the protein. This hypothesis was confirmed by fluorescent binding experiments carried out using recombinant FtsZ in the presence of TL. A high binding affinity was detected for TL toward FtsZ with a Kd value of 17.4± 0.8 nM, supporting the hypothesis that FtsZ is the specifc target of the peptide. This value is lower as compared to the that reported for MciZ (0.3±0.1 μM), the physiological inhibitor of FtsZ (23).

Functional investigation of the TL effect on FtsZ were then performed both *in vitro* and *in vivo*. Enzymatic assays aimed at measuring the GTPase activity of the FtsZ in the presence of TL confirmed that TL is a competitive inhibitor of the protein, as indicated by the docking simulation. Morphologic investigations of *E. coli* cells in the presence of TL by either optical microscopy measurements or TEM analyses revealed the formation of largely elongated "necklace-like" structures originated by a moltitude of bacterial cells, demonstrating that the presence of the peptide hinders *E. coli* cells division. TEM images showed several cells bound together and unable to divide. Consistent with this observation, the results of static light scattering experiments showed the occurrence of elongated structures larger than 6000 nm in the presence of TL.

Analysis of the bacterial cells was also performed by SANS that allows investigation of the morphology and the structure at the nanoscale level. In particular, the atom density distribution of an object is obtained from the analysis of its neutron scattering intensity as function of the scattering vector, q, when illuminated with a neutron beam. Thus, the scattering profile provides structural information over a size scale, d, depending of the q range, according to $d \sim 2\pi/q$. In the present paper, SANS was exploited to investigate the effect of TL on *E. coli* cells, focusing on the structure formed in the range of 2 to 300 nm. According to the literature there are only a few papers presenting such investigation on living cells (24).

Neutron scattering measurements discloses a change in the spatial arrangement of the protein involved in the interaction suggesting that a protein underwent a structural changes following incubation with the peptide in agreement with the docking calculation. Notably, in the intermediate q range, i.e. the range where structural changes on the membrane would be detectable, SANS analyses clearly showed no differences in the lamellar structure of *E.coli* cells, indicating the absence of a destabilization of the bacteria membrane.

Overall our data depicted the following mechanism of action for Temporin L on *E. coli* cells: the peptide crosses the outer membrane of bacteria and specifically binds FtsZ inhibiting its GTPase activity by a competitive inhibition mechanism. This event impairs bacterial cell division resulting in the formation of long cell filaments, and finally bacterial cell death. Due to its haemolytic activity, Temporin L cannot be considered as an effective alternative to common antibiotics, although optimization of the peptide properties by subtle modification of its chemical structure can reduce its haemolytic activity (25). However, elucidation of the mechanism of action at the molecular level pointed out to FtsZ as a possible good target for the rational design of new antibiotics since this protein is responsible for a crucial biological event of bacterial life and is absent in humans.

MATERIALS AND METHODS

The Fmoc amino acids used for the peptide synthesis and 2-(1H-7-Azabenzotriazol-1-yl)-1,1,3,3-tetramethyluronoium hexafluorphosphate (HATU) were purchased from IRIS Biotech GMBH. The Rink amide MBHA resin and the activators N-hydroxybenzotriazole (HOBT) and O-benzotriazole-N,N,N′,N′- tetramethyl-uronium-hexafluoro-phosphate (HBTU) were purchased from Novabiochem (Gibbstown, NJ, USA). Acetonitrile (ACN) was from Romil, dry N,N-dimethylformamide (DMF), 6-[Fluorescein-5(6)-carboxamido]hexanoic acid, N-(+)-Biotinyl-6-aminohexanoic acid and all other reagents were from Sigma Aldrich (MERCK).

Purification was carried out on a Phenomenex Jupiter 10µ Proteo 90 Å (250 × 10 mm) column. Purification was carried out by RP-HPLC with a Shimadzu LC-8A, equipped with a SPD-M10 AV diode array detector using a Kinetex® 5µm C18 100 Å, AXIA Packed LC Column 50 x 21.2 mm, Ea column with a flow rate of 20 $mLmin^{-1}$**.** Peptides were obtained with a purity >95%; yields were calculated based on the amount of peptide obtained after purification.

Peptide Synthesis

Peptides were synthesized on solid phase by Fmoc chemistry on the MBHA (0.54 mmol/g) resin by consecutive deprotection, coupling and capping cycles (26).

Biotin-conjugated TL was obtained by removing the amino terminal Fmoc group and coupling the peptide with N-(+)-Biotinyl-6-aminohexanoic acid in DMF employing the following conditions: 10 equivalents of N-(+)-Biotinyl-6-aminohexanoic acid + 9.8 equivalents of HATU (0.45 M in DMF)+ 14 equivalents of DIPEA; the solution was reacted with the peptide for 3 h at r.t. and double coupling was performed. Peptide was cleaved off the resin and deprotected by treatment with TFA/TIS/H_2O 95/2.5/2.5 v/v/v, 90 min. TFA was concentrated and peptides were precipitated in cold ethylic ether.

Purification of the peptides was performed by semi-preparative RP-HPLC using a gradient of acetonitrile (0.1% TFA) in water (0.1% TFA) from 30 to 85% in 30 min. Products were lyophilized three times and the peptides were characterized by MALDI tandem mass spectrometry (MALDI-MS/MS).

Bacterial cell growth and viability

The minimum inhibitory concentration (MIC) of TL was measured by broth microdilution. The cell strain of *E. coli* BL_{21} was incubated overnight in LB at 37°C. The culture was diluted to obtain a concentration of 0.08 OD_{600} / mL in fresh medium and grown at 37°C for 90 minutes. At an OD/mL value of 0.5, 50 µl of bacterial suspension were added to ten wells and incubated with serial dilutions of the TL peptide from an initial concentration of 512 µM. The sterility control well contained 100 µL of LB, while the growth control well contained 100 µL of microbial suspension. *E. coli* cells were grown as previously described and the MIC was determined by the lowest concentration showing no visible growth after 24 h of incubation at 37°C by measuring the Abs at 600 nm. The assay was performed in triplicate.

Membrane proteins extraction.

E. coli cells were inoculated in 10 mL of liquid LB (*Luria-Bertani*) and placed at 37°C for 16 h under stirring. At the end of the incubation, bacterial cells were grown in 1L at 37°C under stirring for 3h. The pellet was recovered by centrifugation at 4°C for 15 minutes at 5000 rpm and stored at -80°C.

The cell pellet was resuspended in 5 mL of *Cell Lysis Buffer* (20 mMTris-HCl pH 8.0 500 mMNaCl, 4 mM DTT, 1 mM PMSF) and subjected to mechanical lysis by French Press. The sample was then centrifuged at 4°C for 30 minutes at 10000 rpm in order to remove the cell debris and the supernatant recovered was ultracentrifuged for 2 hours at 4°C at 54,000 rpm. The obtained pellet was resuspended in solubilization buffer (50 mMTris-HCl pH 8.0, 500 mMNaCl, 10% Glicerol, 4 mM DTT, 1 mM PMSF, 6 mM 3-[(3-Cholamidopropyl)dimethylammonio]-1-propanesulfonate (CHAPS)) under stirring at 4°C for 16 h. The sample was again ultracentrifuged for 2 hours at 4°C at 54,000 rpm. The supernatant containing cytosolic proteins was removed, while the membrane proteins were dissolved in solubilization buffer.

Pull Down experiments

The pull-down experiment was performed using 200 µL of dry avidin-conjugated agarose beads. The resin was divided in two portions, one portion was left unmodified and the second was incubated with a solution of 2 mg/mL of biotinylated TL for 30 minutes at

4°C under stirring. The supernatant was then removed by centrifugation at 4°C for 10 minutes at 3000 rpm and the resin equilibrated with 5 volumes of binding buffer at 4°C. About 2.5 mg of membrane proteins were incubated on free agarose beads at 4°C for 2h under stirring to remove possible non-specific binding, according to the pre-cleaning procedure. The supernatant containing the unbound membrane proteins was recovered by centrifugation at 4°C for 10 minutes at 3000 rpm and then incubated on agarose beads with the immobilized peptide for 3h at 4°C under stirring. Beads were washed with 5 volumes of binding buffer and the peptide-interacting proteins were released by competitive elution with 500 µL of elution buffer containing an excess of biotin for 1h at 4°C under stirring.

TL putative protein interactors were fractionated by SDS-PAGE. Protein bands from sample and control lanes were excised from the gel and subjected to *in situ* hydrolysis with trypsin. The resulting peptide mixtures were analyzed by Liquid Chromatography/Tandem Mass Spectrometry (LC-MS/MS) using a LTQ Orbitrap XLOrbitrap mass spectrometer (Thermo Fisher Scientific, Bremen, Germany) and the data obtained were used to search for a non-redundant protein database using an in house version of the Mascot software leading to identification of the putative AMP protein interactors. The putative peptide interactors were gathered within functional pathways by bioinformatic tools (DAVID, KEGG, STRING).

Docking calculations

The putative binding site of TL on FtsZ was determined using docking calculations. The structure of Ftsz has been modelled using SwissProt Model Server and the chain A of the structure of the protein from *P. aeruginosa* (2VAW, 60% sequence identity) as starting model (27, 28). The NMR structure of TL was kindly provided by Prof. Surajit Bhattacharyya. The peptide adopts an α-helix structure, in good agreement with CD spectra collected in solution (29). Interestingly, PEP-FOLD3 also predicts a helical structure for this peptide (30).

The model of the FtsZ-TL complex was obtained using FTDOCKs (31). The structure of the complex was then energy minimized and refined using Flexpeptdock (32). We have verified that the peptide binding site was predicted also by other docking programs and indeed the peptide binding site was predicted also by PEPDOCK and SWARMDOCK

(33, 34). Analysis of the structure was done using Coot (35) figures were generated with PyMol (www.pymol.org).

Expression of Escherichia coli FtsZ and enzymatic assay

Untagged *E. coli* FtsZ was expressed from pET28a in BL21 cells. Cells were grown at 37 °C in 200 mL of LB culture media with 50μg/mL kanamycin and 0.4 mM isopropyl-beta-D-thiogalactopyranoside (IPTG) was added at an optical density of ∼0.5 at 600 nm. The culture was grown for 90 min at 37°C for FtsZ production. Cells were harvested by centrifugation (5000 rpm during 15 min at 4 °C), and pellets were resuspended in Tris glycerol buffer (Tris glycerol buffer, 50 mM Tris-HCl, 50 mM KCl, 1 mM EDTA, 10% glycerol, pH 8.0) and were lysed on ice using a sonicator. The soluble fraction, containing the FtsZ protein, was separated from the cell debris by centrifugation (100,000 × g for 2 h at 4 °C).

The protein from the soluble fraction was precipitated with 30% ammonium sulfate for 16h. The sample was centrifuged (10000 rpm for 35 min at 4 °C), and the pellet was resuspended in 5 ml Tris glycerol buffer, pH 8.0 and dialyzed to remove the ammonium sulfate. The sample was purified by anion exchange chromatography using a Mono-Q HR 5/5 column equilibrated with Tris glycerol buffer, pH 8.0. FtsZ was retained on the column and was eluted with a 0–100% gradient of 1 M NaCl in the same buffer (36).

Protein concentration was estimated with Bradford reagent (Bio-Rad protein assay), protein purity was assessed by SDS- polyacrylamide gel electrophoresis (SDS-PAGE) and characterized by mass mapping using MALDI-MS/MS.

The activity of FtsZ on GTP substrate was determined with an enzymatic assay using BIOMOL® Green phosphate reagent (Biomol). Initially, FtsZ (6 μM) was incubated in 25 mM PIPES/NaOH, pH 6.8 for 30 minutes at 30°C. The enzyme was then treated with different concentrations of GTP, ranging from 0 μM to 250 μM, either in the absence or in the presence of 35 μM TL. The reaction was performed for 10 min and then stopped by addition of 100 μl BIOMOL® Green reagent and the increase in absorbance at 620 nm was measured following 25 min incubation. The experiment was performed in duplicate. Kinetic parameters were fitted by non-linear regression with GraphPad Prism 4Project.

Binding experiment

Fluorescence experiments were performed at 25 °C in a 250µL quartz cuvettes (Hellma, Germany) on a VARIAN Cary Eclipse Fluorimeter. Titrations were carried out in 50 mM Tris-HCl buffer pH 7.2, 1M NaCl. Fluo-TL was excited at 440 nm (slit 5 nm) and the emission was monitored at 520 nm (slit 5 nm) without and in the presence of increasing concentrations of FtsZ protein (from 0.003 to 0.121µM) in a High Voltage mode. The peptide and the protein were dissolved at a 1.5 µM concentration. All experiments were repeated in duplicate. The change in the fluorescence intensity of the reaction set was fit into "one site-specific binding" equation of GraphPad Prism 5 (GraphPad Software).

Optical Microscopy and TEM analyses

E. coli cells were inoculated in 10 mL of liquid LB and placed at 37°C for 16 h under stirring. At the end of the incubation, bacterial cells grown to 0.5 OD/mL were incubated with 20 µM TL and allowed to grow for a further 5 h. A similar bacterial growth was prepared and used as control in the absence of the peptide. Samples of 100 µL were observed by optical microscope using a ZEISS optical microscope for phase contrast and 50X magnifications.

For TEM analysis, *E.coli* cells were treated with sub-MIC concentration of TL for 1h at 37°C. After incubation, bacterial cells were centrifugated at 3000rmp for 15min, washed with PBS and resuspended in PBS containing 2.5% glutaraldehyde to fix the cells. Samples (10µl) were applied to a glow discharged formvar/carbon film copper mesh grid and led to adsorb for 2 minutes. The excess liquid was eliminated with water and the sample was stained with 1% uranyl acetate allowing the grids to dry before TEM analyses. TEM analyses were carried out on a JEOL JEM-1400 TEM with an accelerating voltage of 120kV. Digital images were collected with an EMSIS Xarosa digital camera with Radius software.

Scattering Measurements

E. coli cells were grown to 0.5 OD/mL in the presence and in the absence of 20 µM TL up to 1 OD at 600 nm. Cells were then centrifuged at 5000 rpm for 15 min, treated with 0.4% paraformaldehyde for 10 min, washed with deuterated PBS1X for three times and the samples were finally resuspended in deuterated PBS1X.

Dynamic Light Scattering (DLS) measurements were performed by using a home-made instrument composed by a Photocor compact goniometer, a SMD 6000 Laser Quantum 50 mW light source operating at 532.5 nm, a photomultiplier (PMT-120-OP/B) and a correlator (Flex02-01D) from *Correlator.com* (37, 38). All measurements were performed at 25 °C with the temperature controlled through the use of a thermostat bath. All the measurements were performed in triplicate at fixed scattering angle of 90°.

Small Angle Neutron Scattering (SANS) measurements were performed at 25 °C with the KWS-2 diffractometer operated by Julich Centre for Neutron Science at the FRMII source located at the Heinz Maier Leibnitz Centre, Garching (Germany). For all the samples, neutrons with a wavelength of 7 Å and $\Delta\lambda/\lambda \leq 0.1$ were used. A two-dimensional array detector at three different wavelength (W)/collimation (C)/sample-to-detector (D) distance combinations (W 7 Å/C 8 m/D 2 m, W 7 Å/C 8 m/D 8 m, and W 7 Å/C 20 m/ D 20 m) measured neutrons scattered from the samples. These configurations allowed collecting data in a range of the scattering vector modulus q between 0.002 $Å^{-1}$ and 0.4 $Å^{-1}$.

The Usans measurements were performed on KWS-3 at 25 °C. The sample-to-detector distances was 9.5 m with a wavelengths of 5Å ($\Delta\lambda/\lambda$ = 10%) and 12.8 Å ($\Delta\lambda/\lambda$ = 20%), respectively. Both in the case of KWS2 and KWS3 meaurements a 1 mm Helma quartz cells were used.

Acknowledgments

This work is based upon experiments performed at the KWS2 instrument operated by JCNS at the Heinz Maier-Leibnitz Zentrum (MLZ), Garching, Germany. LP is grateful to MLZ for providing beam time. AD thanks prof. Prof. Miguel Vicente Centro Nacional de Biotecnología, Consejo Superior de Investigaciones Científicas, Madrid, Spain for providing *E.coli* cells for FtsZ production. This work was supported in part by MIUR grants ARS01_00597 Project "NAOCON" and PRIN 2017 "Identification and characterization of novel antitumoral/antimicrobial insect-derived peptides: a multidisciplinary, integrated approach from in silico to in vivo".

Conflict of interest

The authors declare that they have no conflicts of interest with the contents of this article.

REFERENCES

1. Le, C. F., Fang, C. M., and Sekaran, S. D. (2017) *Antimicrob Agents Chemother* **61**
2. Marr, A. K., Gooderham, W. J., and Hancock, R. E. (2006) *Curr Opin Pharmacol* **6**, 468-472.
3. Lewies, A., Du Plessis, L. H., and Wentzel, J. F. (2019) *Probiotics Antimicrob Proteins* **11**, 370-381
4. Freire, J. M., Gaspar, D., Veiga, A. S., and Castanho, M. A. (2015) *J Pept Sci* **21**, 178-185
5. Agrawal, A., and Weisshaar, J. C. (2018) *Biochim Biophys Acta Biomembr* **1860**, 1470-1479
6. Avitabile, C., D'Andrea, L. D., and Romanelli, A. (2014) *Sci Rep* **4**, 4293
7. Malgieri, G., Avitabile, C., Palmieri, M., D'Andrea, L. D., Isernia, C., Romanelli, A., and Fattorusso, R. (2015) *ACS Chem Biol* **10**, 965-969
8. Freire, J. M., Gaspar, D., de la Torre, B. G., Veiga, A. S., Andreu, D., and Castanho, M. A. (2015) *Biochim Biophys Acta* **1848**, 554-560
9. Avitabile, C., D'Andrea, L. D., Saviano, M., Olivieri, M., Cimmino, A., and Romanelli, A. (2016) *Biochem Bioph Res Co* **478**, 149-153
10. Yang, Z., and Weisshaar, J. C. (2018) *ACS Chem Biol* **13**, 2161-2169
11. Yadavalli, S. S., Carey, J. N., Leibman, R. S., Chen, A. I., Stern, A. M., Roggiani, M., Lippa, A. M., and Goulian, M. (2016) *Nat Commun* **7**, 12340
12. Vetterli, S. U., Zerbe, K., Muller, M., Urfer, M., Mondal, M., Wang, S. Y., Moehle, K., Zerbe, O., Vitale, A., Pessi, G., Eberl, L., Wollscheid, B., and Robinson, J. A. (2018) *Sci Adv* **4**, eaau2634.
13. Andolina, G., Bencze, L. C., Zerbe, K., Muller, M., Steinmann, J., Kocherla, H., Mondal, M., Sobek, J., Moehle, K., Malojcic, G., Wollscheid, B., and Robinson, J. A. (2018) *ACS Chem Biol* **13**, 666-675.
14. Hagan, C. L., Wzorek, J. S., and Kahne, D. (2015) *Proc Natl Acad Sci U S A* **112**, 2011-2016.
15. Rinaldi, A. C., Mangoni, M. L., Rufo, A., Luzi, C., Barra, D., Zhao, H., Kinnunen, P. K., Bozzi, A., Di Giulio, A., and Simmaco, M. (2002) *Biochem J* **368**, 91-100.
16. Ray, S., Dhaked, H. P., and Panda, D. (2014) *Biochemistry* **53**, 6426-6429.
17. Monti M, Cozzolino M, Cozzolino F, Vitiello G, Tedesco R, Flagiello A, Pucci P. (2009) *Expert Rev Proteomics* **6**, 159-169.
18. G. Chesi, R.N. Hegde, S. Iacobacci, M. Concilli, S. Parashuraman, B.P. Festa, E.V. Polishchuk, G. Di Tullio, A. Carissimo, S. Montefusco, D. Canetti, M. Monti, A. Amoresano, **P. Pucci**, B. van de Sluis, S. Lutsenko, A. Luini and R.S. Polishchuk. (2016) *Hepatology* **63,** 1842-1859.
19. A. Varone, S. Mariggiò, M. Patheja, V. Maione, A. Varriale, M. Vessichelli, D. Spano, F. Formiggini, M. Lo Monte, N. Brancati, M. Frucci, P. Del Vecchio, S. D'Auria, A. Flagiello, C. Iannuzzi, A. Luini, **P. Pucci**, L. Banci, C. Valente and D. Corda. (2019) *Cell Commun Signal* **17**, 20-
20. Kirkpatrick, C. L., and Viollier, P. H. (2011) *Curr Opin Microbiol* **14**, 691-697.

21. Mohammadi, T., Karczmarek, A., Crouvoisier, M., Bouhss, A., Mengin-Lecreulx, D., and den Blaauwen, T. (2007) *Mol Microbiol* **65**, 1106-1121
22. Fenton, A. K., and Gerdes, K. (2013) *Embo J* **32**, 1953-1965.
23. Ray, S., Kumar, A., and Panda, D. (2013) *Biochemistry* **52**, 392-401.
24. Semeraro, E. F., Devos, J. M., Porcar, L., Forsyth, V. T., and Narayanan, T. (2017) *IUCrJ* **4**, 751-757.
25. Setty, S. C., Horam, S., Pasupuleti, M., and Haq, W. (2017) *Int J Pept Res Ther* **23**, 213-225.
26. Piras, L., Avitabile, C., D'Andrea, L. D., Saviano, M., and Romanelli, A. (2017) Biochem Bioph Res Co 493, 126-131.
27. Waterhouse, A., Bertoni, M., Bienert, S., Studer, G., Tauriello, G., Gumienny, R., Heer, F. T., de Beer, T. A. P., Rempfer, C., Bordoli, L., Lepore, R., and Schwede, T. (2018) Nucleic Acids Res 46, W296-W303
28. Oliva, M. A., Trambaiolo, D., and Lowe, J. (2007) J Mol Biol 373, 1229-1242
29. Avitabile, C., D'Andrea, L. D., Saviano, M., and Romanelli, A. (2016) *Rsc Adv* **6**, 51407-51410
30. Shen, Y. M., Maupetit, J., Derreumaux, P., and Tuffery, P. (2014) J Chem Theory Comput 10, 4745-4758
31. Gabb, H. A., Jackson, R. M., and Sternberg, M. J. (1997) J Mol Biol 272, 106- 120
32. Raveh, B., London, N., and Schueler-Furman, O. (2010) Proteins 78, 2029-2040.
33. Lee, H., Heo, L., Lee, M. S., and Seok, C. (2015) Nucleic Acids Res 43, W431- 435
34. Torchala, M., Moal, I. H., Chaleil, R. A., Fernandez-Recio, J., and Bates, P. A. (2013) Bioinformatics 29, 807-809
35. Emsley, P., Lohkamp, B., Scott, W. G., and Cowtan, K. (2010) Acta Crystallogr D Biol Crystallogr 66, 486-501
36. Rivas, G., Lopez, A., Mingorance, J., Ferrandiz, M. J., Zorrilla, S., Minton, A. P., Vicente, M., and Andreu, J. M. (2000) J Biol Chem 275, 11740-11749
37. Della Vecchia, N. F., Luchini, A., Napolitano, A., D'Errico, G., Vitiello, G., Szekely, N., d'Ischia, M., and Paduano, L. (2014) Langmuir 30, 9811-9818
38. Luchini, A., Irace, C., Santamaria, R., Montesarchio, D., Heenan, R. K., Szekely, N., Flori, A., Menichetti, L., and Paduano, L. (2016) Nanoscale 8, 10078-10086

LEGENDS TO THE FIGURES

Figure 1. (A) Distribution of TL putative protein partners identified in the pull-down experiment according to their cellular localization and biological functions. (B) STRING analysis of the putative TL interactors belonging to the divisome complex showing the occurrence of a network including 8 proteins: FtsZ, FtsA, MurG, MukB, Rho, DacA, pea and MreB.

Figure 2. (A) Sequence alignment of peptides Temporin L, CRAMP 16-33 and MciZ. (B) The predicted structure of the complex between FtsZ (yellow) and TL (cyan). (C) Putative binding site well superimposes to that of GDP in the structures of *B. subtilis* and *P. aeruginosa* FtsZ. (D) Predicted binding site of TL (cyan) on FtsZ structure (yellow).

Figure 3. (A) Binding of TL to FtsZ as determined by fluorescence experiments using N-terminal fluoresceine-labelled TL and recombinant FtsZ. (B) Enzymatic activity of recombinant FtsZ in the absence and in the presence of 35 μM TL using GTP as substrate.

Figure 4. Optical microscopy images of *E. coli* cells grown in the absence (panel A) and in the presence (panel B) of 20 μM TL. Long necklace-like structures formed by *E. coli* cells were clearly detected in the presence of the peptide confirming the impairment of bacterial cell division.

Figure 5. TEM analysis of *E. coli* cells grown in the absence (panel A) and in the presence (panel B) of 20 μM TL. TEM images further confirmed the occurrence of bacterial cells unable to divide in the presence of TL (panel B) as compared to the control (panel A).

Figure 6. Dynamic Light Scattering (LS), USANS, and SANS analyses of *E. coli* cells in the absence (black points) and in the presence (red points) of 20 μM TL. LS measurements showed a decrease of the intensity with a q^{-1} power law for the treated sample, whereas this value remained essentially constant for the untreated sample.

SUPPLEMENTARY MATERIAL

The antimicrobial peptide Temporin L impairs *E. coli* cell division by interacting with FtsZ and the divisome complex

Angela Di Somma, Concetta Avitabile, Arianna Cirillo, Antonio Moretta, Antonello Merlino, Luigi Paduano, Angela Duilio and Alessandra Romanelli

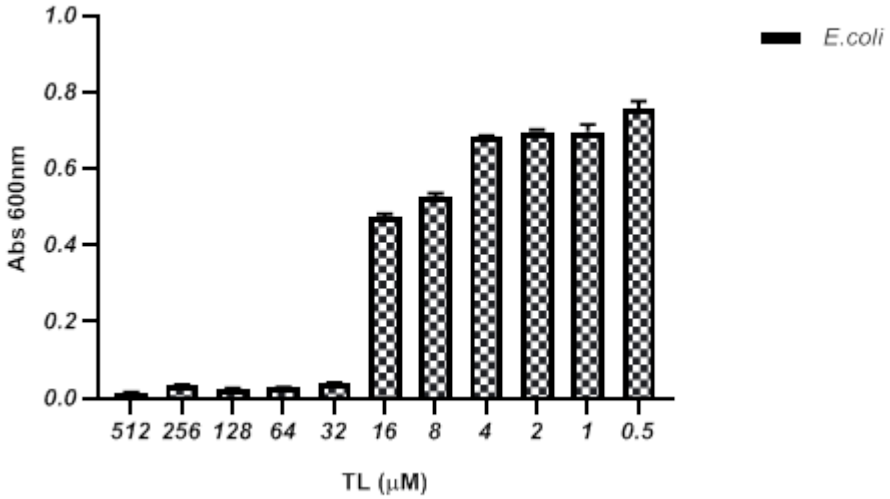

Supplementary Figure 1. Determination of TL minimum inhibitory concentration (MIC). *E. coli* cells were grown in the presence of serial dilution of TL from 512 μM to 0.5 μM and MIC was determined by the lowest concentration showing no visible growth after 24h of incubation at 37°C. Measurements were performed in triplicate.